Letter

Extracting model-independent nuclear level densities away from stability

D. Mücher,[1,2,3,*] A. Spyrou,[4,5,6,†] M. Wiedeking,[7,8] M. Guttormsen,[9] A. C. Larsen,[9] F. Zeiser,[9] C. Harris,[10,5] A. L. Richard,[10,6] M. K. Smith,[10] A. Görgen,[9] S. N. Liddick,[10,11] S. Siem,[9] H. C. Berg,[10,5] J. A. Clark,[12] P. A. DeYoung,[13] A. C. Dombos,[14] B. Greaves,[1] L. Hicks,[10,5] R. Kelmar,[14] S. Lyons,[15] J. Owens-Fryar,[10,5] A. Palmisano,[10,5] D. Santiago-Gonzalez,[12] G. Savard,[12] and W. W. von Seeger[13]

[1]*Department of Physics, University of Guelph, Guelph, Ontario N1G 2W1, Canada*
[2]*Institut für Kernphysik der Universität zu Köln, Zülpicher Strasse 77, D-50937 Köln, Germany*
[3]*TRIUMF, 4004 Wesbrook Mall, Vancouver, British Columbia V6T 2A3, Canada*
[4]*Facility for Rare Isotope Beams, Michigan State University, East Lansing, Michigan 48824, USA*
[5]*Department of Physics & Astronomy, Michigan State University, East Lansing, Michigan 48824, USA*
[6]*Joint Institute for Nuclear Astrophysics, Michigan State University, East Lansing, Michigan 48824, USA*
[7]*Department of Subatomic Physics, iThemba LABS, P.O. Box 722, Somerset West 7129, South Africa*
[8]*School of Physics, University of the Witwatersrand, Johannesburg 2050, South Africa*
[9]*Department of Physics, University of Oslo, NO-0316 Oslo, Norway*
[10]*National Superconducting Cyclotron Laboratory, Michigan State University, East Lansing, Michigan 48824, USA*
[11]*Department of Chemistry, Michigan State University, East Lansing, Michigan 48824, USA*
[12]*Physics Division, Argonne National Laboratory, Argonne, Illinois 60439, USA*
[13]*Department of Physics, Hope College, Holland, Michigan 49422-9000, USA*
[14]*Department of Physics, University of Notre Dame, Notre Dame, Indiana 46556, USA*
[15]*Pacific Northwest National Laboratory, Richland, Washington 99352, USA*

(Received 20 July 2022; accepted 6 December 2022; published 11 January 2023)

The nuclear level density (NLD) is a fundamental measure of the complex structure of atomic nuclei at relatively high energies. Here we present the first model-independent measurement of the absolute partial NLD for a short-lived nucleus. For this purpose we adapt the recently introduced "shape method" for β-decay experiments, providing the shape of the γ-ray strength function for exotic nuclei. In this work, we show that combining the shape method with the β-Oslo technique allows for the extraction of the NLD of the populated states without the need for theoretical input. This development opens the way for the extraction of experimental NLDs far from stability with major implications in astrophysical and other applications. We benchmark our approach using data for the stable ^{76}Ge nucleus, finding excellent agreement with previous experimental results. In addition, we present new experimental data and determine the absolute partial level density for the short-lived ^{88}Kr nucleus. Our results suggest a fivefold increase in the NLD for the case of ^{88}Kr, compared to the recommended values from semimicroscopic Hartree-Fock Bogoliubov calculations recommended by the RIPL3 nuclear data library. However, our results are in good agreement with other semimicroscopic level density models. We demonstrate the impact of our method on the ^{87}Kr(n,γ) neutron capture rate and show that our experimental uncertainties for NLDs fulfill the requirements needed for astrophysical calculations predicting r-process abundances.

DOI: 10.1103/PhysRevC.107.L011602

I. INTRODUCTION

Nuclei are complex quantum many-body systems. For low-excitation energies, their structure can be described using the properties (energy, spin, parity, width) of individual levels. However, moving to higher energies, where the levels get closer and overlap, these properties need to be combined into a statistical description of the nucleus [1]. One of the most important statistical properties is the NLD as it carries information about the structure of the nucleus, such as pair breaking, shell effects, shape changes, and collectivity. In addition, the NLD is a critical input in nuclear reaction calculations, in particular for neutron-capture reaction cross sections and neutron-induced fission calculations. These reactions provide pivotal input for nuclear astrophysics and applications in nuclear energy and security [2–6].

In 1936, Bethe first described the nucleus as a group of noninteracting fermions [7,8]. Since then modern approaches were developed which are typically semi-microscopic, e.g., [9–12], or shell-model based, e.g., [13–17]. While effective shell model calculations are a powerful tool to describe NLDs within a local area of the nuclear chart, semimicroscopic approaches are preferred for large scale calculations, such as calculating neutron-capture rates on nuclei far from stability,

*dmuecher@ikp.uni-koeln.de
†spyrou@frib.msu.edu

e.g., for the astrophysical r process [18], and for nuclear energy production [5,6].

Available semimicroscopic NLD models use the Hartree-Fock-Bogoliubov (HFB) plus combinatorial approach [19,20] to extract energy-, spin-, and parity-dependent NLDs [10–12]. They reproduce existing experimental data along the valley of stability, within two normalization factors, α (slope) and δ (offset):

$$\rho(E_x, J, \pi) = e^{\alpha\sqrt{E_x-\delta}}\rho(E_x-\delta, J, \pi), \tag{1}$$

where ρ is the NLD as a function of excitation energy E_x, spin J, and parity π. A detailed study [11,12] of the α and δ normalization parameters for 289 nuclei showed that the values of the two parameters are centered around zero, but can also deviate significantly from zero with major implications on the absolute value of the NLD and, as a result, the neutron-capture reaction rates.

Experimentally, measurements of the NLD are limited to stable nuclei or their closest neighbors. Commonly used techniques for extracting the NLD around stability are the Oslo method [21–23], the particle-evaporation method [24,25], and the direct measurement of neutron-resonance spacings close to the neutron-separation energy. New experimental techniques were developed that can provide NLDs on short-lived nuclei (β-Oslo [26], inverse-Oslo [27]). However, all Oslo-type techniques that can be applied to short-lived nuclei rely on inputs from theoretical models. Here we present the first model-independent approach for extracting a partial NLDs for short-lived nuclei.

II. METHOD: DETERMINING ABSOLUTE PARTIAL LEVEL DENSITIES

In the present work we make use of the β-Oslo method [26] and combine it with the recently introduced "shape method" [28] to eliminate any model dependencies in the extraction of NLDs. In the β-Oslo method, the nucleus of interest is populated via β decay, allowing one to do experiments with nuclei far from stability, where the secondary beam intensities can be as low as 1 pps [26,29]. A segmented total absorption spectrometer is used to simultaneously measure the excitation energy and individual γ-ray transitions of the populated nucleus. Following the unfolding of the data with the detector response [23], an iterative subtraction process allows for the extraction of the first generation γ rays as a function of excitation energy, E_x [22]. The extracted first generation (primary) γ-ray matrix $P(E_x, E_\gamma)$ can be factorized as [21]:

$$P(E_x, E_\gamma) \propto T(E_\gamma)\rho(E_x - E_\gamma), \tag{2}$$

where $\rho(E_x - E_\gamma)$ is the NLD at the excitation energy after the first γ-ray is emitted and $T(E_\gamma)$ is the transmission coefficient for γ emission. In β-decay experiments, $\rho(E_x - E_\gamma)$ is a partial NLD, which includes spins that correspond to the assumed allowed β-decay transitions, followed by a dipole γ-ray emission. Consequently, $T(E_\gamma)$ corresponds to γ emission of dipole nature. An infinite number of solutions are possible for the above equation [21], and the physical solution is obtained when normalizing the $\rho(E_x - E_\gamma)$ and $T(E_\gamma)$ to known data with

$$\begin{aligned}\rho'(E_x - E_\gamma) &= Ae^{\tilde{\alpha}(E_x-E_\gamma)}\rho(E_x - E_\gamma)\\ T'(E_\gamma) &= Be^{\tilde{\alpha}(E_\gamma)}T(E_\gamma),\end{aligned} \tag{3}$$

where A and B are constants and $\tilde{\alpha}$ is a common slope parameter. Typical normalization data used in the Oslo method are (1) low-lying discrete levels, (2) the level density at the neutron separation energy, $\rho(S_n)$, calculated from neutron-resonance spacing, D_0, data where available, and (3) the average total radiative width $\langle\Gamma_\gamma\rangle$ at S_n. When dealing with unstable nuclei, typically the low-lying discrete levels are available, and the magnitude of the γ-ray strength function (γSF) can be constrained using Coulomb dissociation measurements in inverse kinematics [29–33]. However, the second normalization point that constrains the NLD at the neutron-separation energy, as well as the slope of both the NLD and the γSF, cannot be provided experimentally for exotic nuclei. Consequently, the absolute values of NLDs for unstable nuclei rely on theory, alone. To eliminate this problem we combine here, for the first time, the β-Oslo method with the shape method [28].

The shape method yields the energy-dependence or "shape" of the γSF, i.e. the γSF up to an absolute normalization constant, in a model-independent way. The traditional shape method [34,35] uses particle-γ-γ data to determine the excitation energy of the nucleus and the feeding to individual discrete levels of the same spin and parity. Through this, the dependence of the γSF on E_γ is determined for each excitation energy E_x. The different data points that correspond to each excitation energy are then combined to extract the complete shape of the γSF. Note that the γSF is assumed to be independent of the excitation energy in any given nucleus for the excitation energies of interest (Brink hypothesis [36]). Here, we apply the shape method to β-decay data. In this case, the excitation energy is extracted from the sum of the total amount of energy deposited in the segmented total absorption spectrometer SuN [37], and the individual γ-ray energy is taken from each segment of the detector (Fig. 1). The shape method relies on the observation of statistical γ ray decays from the quasicontinuum into discrete, low-lying levels, L_j, with energies E_{L_j}. We assume that the primary γ decays into the states, L_j, will be dominated by dipole transitions [38]. In the present work we restrict the analysis to two discrete states with identical spin, $L_{1,2} = 2^+_{1,2}$, in the even-even daughter nucleus. These transitions appear in our data as diagonals in a two-dimensional (2D) matrix with excitation energy on the y axis and γ-ray energy on the x axis, e.g., Fig. 1. We use projections of the 2D matrix along the diagonals $(E_x - E_\gamma)$, as shown in the same figure, for different excitation energies and extract the γ-ray intensities N_{L_j} into the states of interest L_j. The ratio of the intensities, N_{L_j}, along the diagonals, corrected for the detector response, is related to the ratio R of the γSFs, $f(E_\gamma)$, for a given energy range E_x [34]:

$$R = \frac{f\left(E_{x,i} - E_{L_1}\right)}{f\left(E_{x,i} - E_{L_2}\right)} = \frac{N_{L_1}(E_{x,i})\left(E_{x,i} - E_{L_2}\right)^3}{N_{L_2}(E_{x,i})\left(E_{x,i} - E_{L_1}\right)^3}. \tag{4}$$

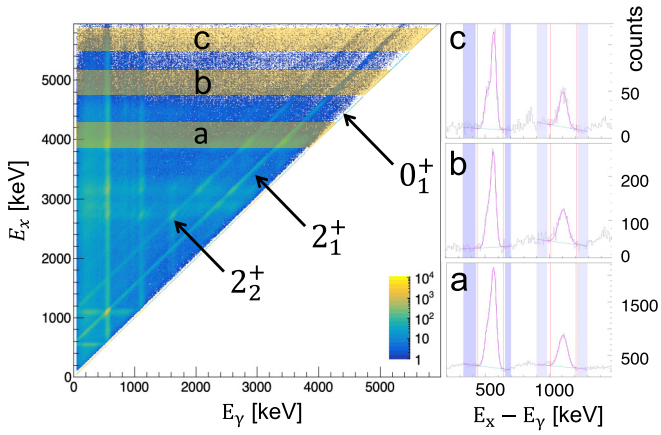

FIG. 1. Left: Raw matrix of excitation energy vs γ-ray energy in SuN after population of ^{76}Ge. Right: Projections along the diagonal, $E_x - E_\gamma$, for three different energy bins (all in keV) $3900 < E_x < 4400$ (a), $4700 < E_x < 5100$ (b), $5500 < E_x < 5900$ (c). The peaks at 563 keV and 1108 keV correspond to decays into the states 2_1^+ and 2_2^+, respectively. The purple shaded areas were used to define a linear background under each peak.

Equation (4) can be applied for n energy ranges with centroids $E_{\min} < E_{x,i} < Q_\beta$ and widths $\Delta E_{x,i}$, with $E_{\min}$ representing the minimum energy at which the population and γ decay of the daughter nucleus behave statistically, and Q_β being the Q value of the β decay. The E_γ^3 correction is based on the assumption that the transitions are of dipole nature.

The γSF is obtained via a "sewing" approach, where the pairs of data points from each excitation energy bin are normalized to each other via linear interpolation [28]. In this work we use a "symmetric sewing" approach in which the vertical distance of data points to the linear interpolation of the neighboring pair of data points is equal. We found the symmetric sewing algorithm to reliably reproduce test input data with similar characteristics to the experimental data and found that the induced uncertainties are small compared to the uncertainties induced by the fluctuations in the experimental spectra. After interpolation, the n pairs of values, $f(E_\gamma)$, reflect the shape of the γSF of the final nucleus.

In the present work the shape method and the β-Oslo technique are combined for the first time to extract a model-independent partial NLD.

III. EXPERIMENTAL VALIDATION

The technique was applied to previously published data for the stable nucleus ^{76}Ge that is fed from the β-decay of ^{76}Ga [26,39]. The original experiment was performed at the National Superconducting Cyclotron Laboratory, at Michigan State University using the Summing NaI (SuN) detector [26,37,39].

Figure 1 (left) shows the raw 2D matrix created from the SuN detector data by using the total deposited energy to determine E_x on the y axis and the individual segments to obtain E_γ on the x axis. The diagonals from the feeding of the first two excited states, 2_1^+ and 2_2^+, from higher lying states in ^{76}Ge are clearly seen, shifted by 563 and 1108 keV, respectively, from the 0_1^+ ground state. A dedicated software program SHAPEIT [40] was developed for this analysis.

Projections of the 2D matrix along the diagonal were created for n bins with constant widths ΔE_{x_i} [Fig. 1 (right)]. The projections are shown with $E_x - E_\gamma$ on the x axis. Peaks belonging to decays into $L_j = (2_1^+, 2_2^+)$ were fit using a Gaussian with a linear background. In the case of decays into the 2_1^+ state, peaks were fit as doublets with the close-lying first-escape peak at $E_x - E_\gamma = 511$ keV. For each excitation energy $E_{x,i}$, the γSF-weighted average energy was determined and ratios of values $f(E_\gamma)$ were calculated using Eq. (4). Applying the above described sewing approach, the shape of the γSF was determined.

In this work we investigate to what extent the results of the shape method behave statistically and are robust with respect to the details of the analysis. Hence, we expanded upon the analysis technique presented in [28] and repeated the "sewing" analysis for a range of energy bins $E_{x,i}$ with varying widths $400 \leqslant \Delta E_{x,i} \leqslant 800$ keV in steps of 50 keV and varying bin positions in steps of 50 keV. To display absolute values, each individual γSF is scaled via χ^2 minimization to the γSF from the β-Oslo analysis using the actual full range of γ-ray energies. For the final display of the γSF values, the convolution of all iterations is averaged over a fixed energy bin of 250 keV. The error for each bin includes both the statistical uncertainties as well as the standard deviation of γSF values of all iterations. The statistical uncertainties are included in the Monte Carlo process, and they are small compared to the error due to matching the γSFs of all iterations

Figure 2 (top) shows the resulting γSF of ^{76}Ge (blue triangles) compared to the results of the β-Oslo method [26], as well as the Oslo results for ^{74}Ge [41]. It should be noted that the original publication for ^{76}Ge using the β-Oslo method used systematics and theoretical calculations to determine the slope of the NLD and consequently the shape of the γSF. The shape method provides here a purely experimental approach to extracting the shape of the γSF. Once the slope of the γSF is extracted we combine the result with the β-Oslo method to extract the NLD via a Monte Carlo approach. In each Monte Carlo iteration, the shape method analysis is performed based on a randomized set of integration bins and positions. Before sewing, for each data point the γSF value is randomized following its statistical error bar. In the next step of the Monte Carlo iteration the γSF from the β-Oslo method is transformed via Eq. (3) to best match the γSF of the shape method. This χ^2 fit of the $\tilde{\alpha}$ parameter is performed within a randomized γ-ray energy range with a lower energy between 3.0 and 4.0 MeV, while no cutoff is applied at high γ ray energies. The Monte Carlo approach finally results in a near-Gaussian distribution of $\tilde{\alpha}$ values, providing a mean value and σ for this parameter.

Compared to the original β-Oslo analysis, the change in the slope, $\delta\tilde{\alpha}$, is 0.05(13). The corresponding absolute partial NLD is shown in Fig. 2 (bottom). The good agreement of both the γSF and level densities to literature values serves as a robust test of our approach and shows that the chosen level density at the neutron separation energy in [26] agrees with our absolute result.

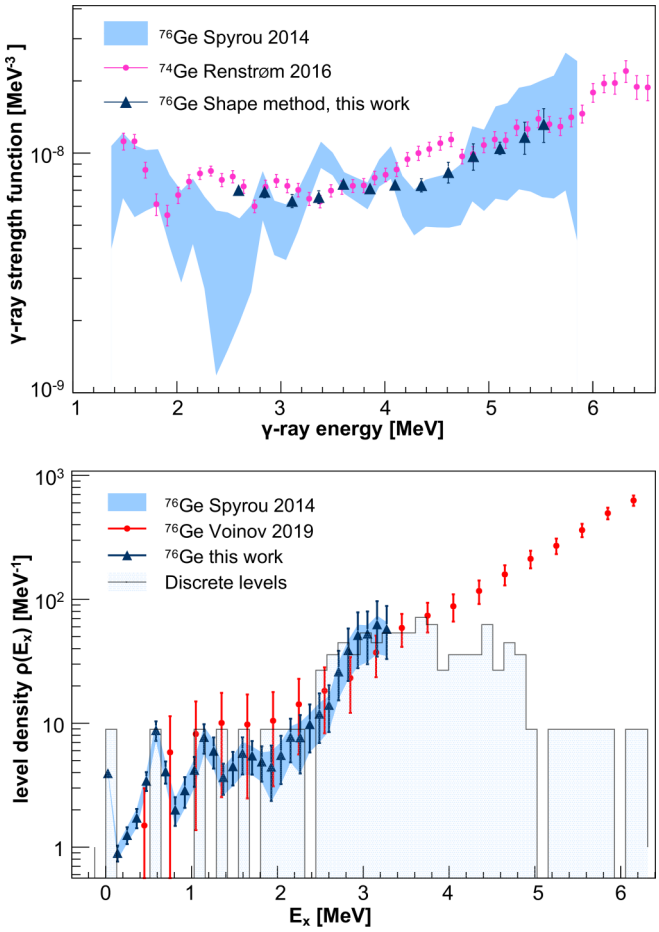

FIG. 2. γSF (top) and total NLD (bottom) for ^{76}Ge. Results from the original publication [26] for ^{76}Ge (blue bands) assume a specific level density $\rho(S_n)$ at the neutron separation energy from theory and systematics, whereas the present results (blue triangles) are model independent. In both cases the NLD populated in the experiment includes spins 0 through 4, assuming allowed β-decay transitions from the 2^- ground state of ^{76}Ga and dipole γ-ray emission. Our results are also in good agreement with the NLD extracted from the particle evaporation method [42] (red circles, bottom). The γSF is also compared to that of ^{74}Ge extracted from the stable beam Oslo method [41] (pink circles, top) in a broader energy range.

IV. FIRST APPLICATION ON AN UNSTABLE NUCLEUS

Following the successful validation of our new approach we applied the shape method to the unstable nucleus ^{88}Kr. The new experiment was performed at the CARIBU [43] facility at Argonne National Laboratory. A ^{88}Br beam was implanted into the SuNTAN tape transport system [44] at the center of the SuN detector decaying into the nucleus ^{88}Kr. Isobar contaminants and daughter activity were removed from the data by using appropriate tape cycles due to their different half-lives compared to ^{88}Br. Surrounding the implantation point, a 3-mm-thick plastic scintillator barrel was used to detect the emitted β particles. The signals from the plastic barrel were collected by 32 wavelength-shifting optical fibers and read by two photomultiplier tubes outside of SuN.

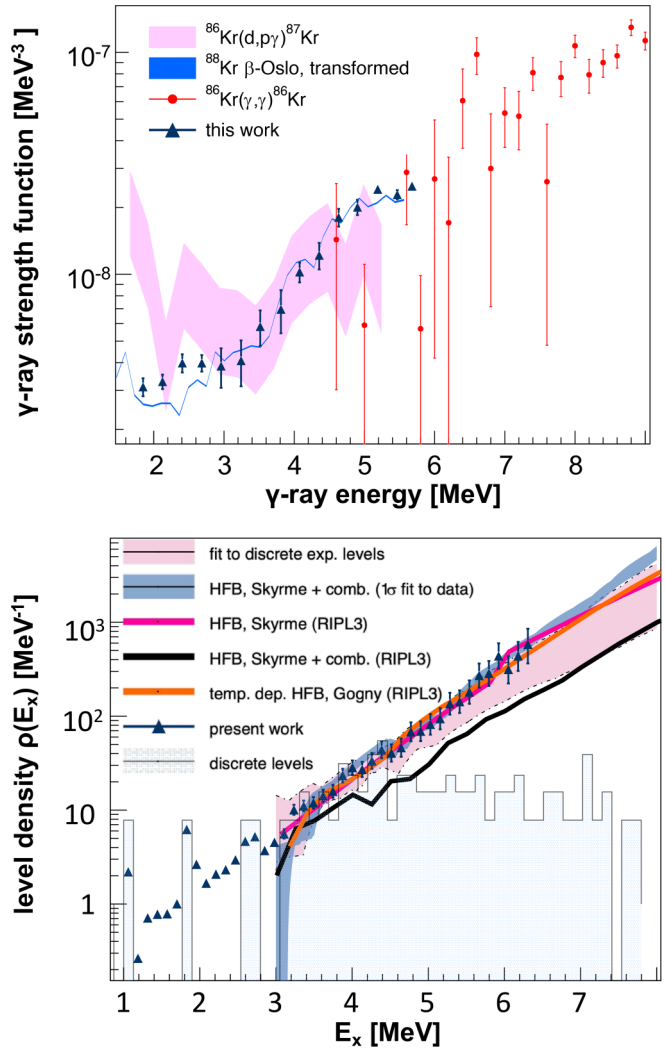

FIG. 3. Top: γSF for ^{88}Kr determined in this work using the shape method (blue triangles). Also shown is the γSF using the β-Oslo technique (blue thin band, statistical uncertainties, only), transformed via Eq. (3) to best match the blue triangles. Our results are scaled to the literature data to guide the eye and allow a comparison of the general trend to data for ^{86}Kr [45] (red circles) and to data for ^{87}Kr (pink band) [27]. Bottom: Measured absolute partial level density for ^{88}Kr (blue triangles) for the spins populated after β decay from ^{88}Br. The blue band is a 1σ uncertainty range, see Sec. V for details. Recommended values from RIPL3 [11,46] are shown as a black line, whereas two additional semimicroscopic models [10,12] are shown in purple and orange solid lines, respectively (see text for details). The pink band shows model predictions [11], constrained via the known discrete levels, only.

The same analysis procedure that was outlined for ^{76}Ge was applied for ^{88}Kr using the diagonals corresponding to $L_j = (2_1^+, 2_2^+)$ at energies 775 and 1577 keV, respectively. The resulting γSF of all analysis iterations, averaged over a fixed bin size of 320 keV, is shown in Fig. 3 (blue triangles, top), and is compared to measurements of other neutron-rich krypton isotopes [27,45]. Within the limitations of the large uncertainties in the previous measurements, the general shape of the γSF is in good agreement.

Following the same procedure as in ^{76}Ge, the transformed β-Oslo results are shown in the thin blue band of Fig. 3 (top). Note that we only display the statistical uncertainties in case of the β-Oslo analysis, as the systematic uncertainties due to the normalization of γSF and ρ are not relevant for the fitting procedure. The absolute partial level density for ^{88}Kr for the states populated in β decay, i.e., of both parities, is shown in the bottom of Fig. 3 (blue triangles). The extracted NLD was normalized to the discrete levels in the 0–3.4 MeV range.

V. COMPARISON TO NUCLEAR LEVEL DENSITY MODELS

In Fig. 3 (bottom) the NLD experimental results are compared to calculations done with three semi-microscopic models: HFB + Skyrme by Goriely *et al.* [10], HFB + Skyrme combinatorial by Goriely *et al.* [11], and temperature-dependent HFB+ Gogny by Hilaire *et al.* [12]. It can be observed that two of the models agree well with our experimental results, while the HFB + Skyrme combinatorial model falls significantly under the data. As mentioned in the introduction, two normalization parameters are used in these models to match experimental data [Eq. (1)]: a slope α and an offset δ. We therefore investigate further the HFB + Skyrme combinatorial model, which is recommended by the RIPL3 [46] database, by adjusting these two parameters.

In the original publication the authors of the HFB + Skyrme combinatorial model performed a study using 289 nuclei for which experimental NLDs were available and presented the overall values of the α and δ parameters (Fig. 8 of Ref. [11]). Using 90% confidence levels the two parameters are within the limits of $-0.7 \leqslant \alpha \leqslant +0.7$ and $-1.1 \leqslant \delta \leqslant +1.1$ MeV. It is important to note that the deviation of the α and δ parameters does not follow any systematic trend (as a function of Z or A of nuclei). Due to the limited knowledge of discrete levels in ^{88}Kr, no slope (α) parameter is recommended [46]. Following Ref. [46] the experimental level scheme in ^{88}Kr is considered complete up to 3.8 MeV. Levels outside of the populated spin range 0–3 were excluded, however, if the spin of a level was not known, that level was still included in this analysis. Using the known discrete levels between 2 and 3.8 MeV, we varied the slope within the above mentioned 90% confidence levels and, in each step, determined the best shift parameter δ. The resulting uncertainty is displayed as a pink band in Fig. 3 (bottom). The recommended level density [46], which has $\alpha = 0$ [Fig. 3 (bottom), black line], is at the lower end of our discrete level fits. This indicates that likely even levels at higher energies have been taken into account when determining δ in [46].

Our result for the absolute partial level density allows us to fit new recommended values for α and δ using the HFB + Skyrme combinatorial model recommended by RIPL-3. For the extraction of an uncertainty for those parameters we again followed a Monte Carlo approach; this time, in each iteration values for ρ were randomized based on the experimental uncertainty at each data point. Then, in each iteration, best values for α and δ are determined for the HFB + Skyrme combinatorial model in comparison to the data. The blue band in Fig. 3 represents a 1σ uncertainty band displaying the model predictions for the best 2/3 (66%) in the $\alpha - \delta$ plane.

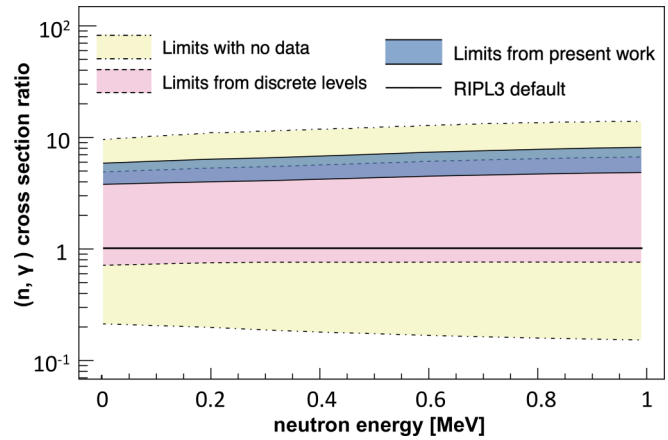

FIG. 4. Neutron-capture cross section ratios relative to values using the RIPL3 recommended level densities [46] (black solid line) in comparison to using the experimental level density from this work (blue band); see Sec. VI for details. Uncertainties for the case of no known discrete levels are shown in yellow, whereas uncertainties achieved using the experimental discrete levels are shown in pink. All calculations were done using the same parameters in TALYS with the exception of the NLD model.

VI. IMPACT ON NEUTRON-CAPTURE REACTION RATES

The nuclear level density is a critical input in neutron-capture reaction rate calculations. Therefore, we investigate the impact of the extracted α and δ parameters discussed in Sec. V for the HFB + Skyrme combinatorial model [11]. For this study we use the TALYS code [47], with all the default parameters and only varying the NLD. We plot our results as ratios compared to the default values of the aforementioned NLD model (Fig. 4). In the figure, the yellow band corresponds to a completely unconstrained NLD using the 90% confidence levels in the α and δ parameters mentioned in Sec. V. In this case the predictions vary by almost two orders of magnitude, even when using a single NLD model. However, even a relatively minor knowledge of discrete levels up to approximately 4 MeV in ^{88}Kr leads to a reduction of this uncertainty by about one order of magnitude, as shown by the pink band in Fig. 4. Using the NLD displayed by the blue band in Fig. 3 of the present work provides a much narrower band of neutron-capture cross section predictions (blue band).

It should be noted that, while the present work provides only the partial NLD for spins $J = 0$–3 of both parities, the conversion to a full NLD does not induce significant additional uncertainty; the six NLD models available in TALYS predict that our spin range corresponds to 33–42% of the full NLD.

VII. CONCLUSIONS

In summary, we have shown that the recently developed shape method [28] delivers robust results for the γSF in unstable nuclei following β decay. In combination with the

β-Oslo method, we were able to extract a model-independent NLD for the partial spin range populated in ^{76}Ge and unstable ^{88}Kr. Thanks to the sensitivity of the β-Oslo technique in combination with the shape method, our error bars are comparable with those achieved using the Oslo method in stable beam experiments. This opens up a new avenue to study the partial NLDs of a large number of unstable nuclei far away from stability, with major impacts on our understanding of nuclear structure, nuclear astrophysics, and nuclear applications. The NLD uncertainties achieved in this work are within the required uncertainties for neutron-capture rates for the *r* process [29] in the case where other input parameters of Hauser-Feshbach calculations, like the absolute γ ray strength function and optical model parameters, are constrained about equally well. We also point out that already the measurement of relatively few discrete levels in a nucleus achieves a reduction in neutron-capture rate uncertainties of one order of magnitude. Hence, future decay experiments with either high-resolution or total-absorption spectrometers at the next-generation radioactive ion beam facilities using beam rates as low as a few particles per second will allow the acquisition of highly sought after information on neutron-capture rates in the *r* process [18].

ACKNOWLEDGMENTS

The authors would like to thank Stephane Goriely for fruitful discussions in the comparison with the theoretical models. The authors acknowledge support of the operations staff at the National Superconducting National Laboratory and at the ATLAS facility at Argonne National Laboratory. This research was partially supported by the Natural Sciences and Engineering Research Council (NSERC) of Canada. The work was supported by the National Science Foundation under Grants No. PHY 1913554, No. PHY 1350234, No. PHY 1430152, No. PHY 1565546, and No. PHY 1613188. This work was supported by the U.S. Department of Energy (DOE) National Nuclear Security Administration Grant No. DOE-DE-NA0003906 and the DOE Office of Science under Grant No. DE-SC0020451. This material is based upon work supported by the Department of Energy/National Nuclear Security Administration through the Nuclear Science and Security Consortium under Award No. DE-NA0003180. D.M. gratefully acknowledges funding by the FRIB Visiting Scholar Award for Experimental Science 2021. A.C.L. gratefully acknowledges funding by the European Research Council through ERC-STG-2014 under Grant Agreement No. 637686, and support from the "ChETEC" COST Action (CA16117), supported by COST (European Cooperation in Science and Technology). This work is based on the research supported in part by the National Research Foundation of South Africa (Grant No. 118846). This material is based upon work supported by the U.S. Department of Energy, Office of Science, Office of Nuclear Physics, under Contract No. DE-AC02-06CH11357. S.L. was supported by the Laboratory Directed Research and Development Program at Pacific Northwest National Laboratory operated by Battelle for the U.S. Department of Energy. This work is partly supported by the Research Council of Norway (Grants No. 263030 and No. 325714).

[1] N. Bohr, Nature (London) **137**, 344 (1936).
[2] P. Fong, Phys. Rev. **89**, 332 (1953).
[3] M. Rajasekaran and V. Devanathan, Phys. Rev. C **24**, 2606 (1981).
[4] A. Larsen, A. Spyrou, S. Liddick, and M. Guttormsen, Prog. Part. Nucl. Phys. **107**, 69 (2019).
[5] G. Aliberti, G. Palmiotti, M. Salvatores, T. Kim, T. Taiwo, M. Anitescu, I. Kodeli, E. Sartori, J. Bosq, and J. Tommasi, Ann. Nucl. Energy **33**, 700 (2006).
[6] N. Colonna, F. Belloni, E. Berthoumieux, M. Calviani, C. Domingo-Pardo, C. Guerrero, D. Karadimos, C. Lederer, C. Massimi, C. Paradela, R. Plag, J. Praena, and R. Sarmento, Energy Environ. Sci. **3**, 1910 (2010).
[7] H. A. Bethe, Phys. Rev. **50**, 332 (1936).
[8] H. A. Bethe, Rev. Mod. Phys. **9**, 69 (1937).
[9] N. Q. Hung, N. D. Dang, and L. T. Q. Huong, Phys. Rev. Lett. **118**, 022502 (2017).
[10] S. Goriely, F. Tondeur, and J. Pearson, At. Data Nucl. Data Tables **77**, 311 (2001).
[11] S. Goriely, S. Hilaire, and A. J. Koning, Phys. Rev. C **78**, 064307 (2008).
[12] S. Hilaire, M. Girod, S. Goriely, and A. J. Koning, Phys. Rev. C **86**, 064317 (2012).
[13] S. Karampagia and V. Zelevinsky, Phys. Rev. C **94**, 014321 (2016).
[14] M. T. Mustonen, N. Gilbreth, Y. Alhassid, and G. F. Bertsch, Phys. Rev. C **98**, 034317 (2018).
[15] W. E. Ormand and B. A. Brown, Phys. Rev. C **102**, 014315 (2020).
[16] Y. Alhassid, G. F. Bertsch, C. N. Gilbreth, and H. Nakada, Phys. Rev. C **93**, 044320 (2016).
[17] N. Shimizu, Y. Utsuno, Y. Futamura, T. Sakurai, T. Mizusaki, and T. Otsuka, Phys. Lett. B **753**, 13. (2016).
[18] M. Mumpower, R. Surman, G. C. McLaughlin, and A. Aprahamian, Prog. Part. Nucl. Phys. **86**, 86 (2016).
[19] S. Hilaire, J. Delaroche, and A. Koning, Nucl. Phys. A **632**, 417 (1998).
[20] Y. Alhassid, S. Liu, and H. Nakada, Phys. Rev. Lett. **83**, 4265 (1999).
[21] A. Schiller, L. Bergholt, M. Guttormsen, E. Melby, J. Rekstad, and S. Siem, Nucl. Instrum. Methods Phys. Res., Sect. A **447**, 498 (2000).
[22] M. Guttormsen, T. Ramsøy, and J. Rekstad, Nucl. Instrum. Methods Phys. Res., Sect. A **255**, 518 (1987).
[23] M. Guttormsen *et al.*, Nucl. Instrum. Methods A **374**, 371 (1997).
[24] A. Wallner, B. Strohmaier, and H. Vonach, Phys. Rev. C **51**, 614 (1995).
[25] A. V. Voinov, S. M. Grimes, U. Agvaanluvsan, E. Algin, T. Belgya, C. R. Brune, M. Guttormsen, M. J. Hornish, T. Massey,

G. E. Mitchell, J. Rekstad, A. Schiller, and S. Siem, Phys. Rev. C **74**, 014314 (2006).
[26] A. Spyrou, S. N. Liddick, A. C. Larsen, M. Guttormsen, K. Cooper, A. C. Dombos, D. J. Morrissey, F. Naqvi, G. Perdikakis, S. J. Quinn, T. Renstrøm, J. A. Rodriguez, A. Simon, C. S. Sumithrarachchi, and R. G. T. Zegers, Phys. Rev. Lett. **113**, 232502 (2014).
[27] V. W. Ingeberg, S. Siem, M. Wiedeking, K. Sieja, D. L. Bleuel, C. P. Brits, T. D. Bucher, T. S. Dinoko, J. L. Easton, A. Görgen, M. Guttormsen, P. Jones, B. V. Kheswa, N. A. Khumalo, A. C. Larsen, E. A. Lawrie, J. J. Lawrie, S. N. T. Majola, K. L. Malatji, L. Makhathini *et al.*, Eur. Phys. J. A **56**, 68 (2020).
[28] M. Wiedeking, M. Guttormsen, A. C. Larsen, F. Zeiser, A. Görgen, S. N. Liddick, D. Mücher, S. Siem, and A. Spyrou, Phys. Rev. C **104**, 014311 (2021).
[29] S. N. Liddick, A. Spyrou, B. P. Crider, F. Naqvi, A. C. Larsen, M. Guttormsen, M. Mumpower, R. Surman, G. Perdikakis, D. L. Bleuel, A. Couture, L. C. Campo, A. C. Dombos, R. Lewis, S. Mosby, S. Nikas, C. J. Prokop, T. Renstrom, B. Rubio, S. Siem, and S. J. Quinn, Phys. Rev. Lett. **116**, 242502 (2016).
[30] D. M. Rossi, P. Adrich, F. Aksouh, H. Alvarez-Pol, T. Aumann, J. Benlliure, M. Böhmer, K. Boretzky, E. Casarejos, M. Chartier, A. Chatillon, D. Cortina-Gil, U. Datta Pramanik, H. Emling, O. Ershova, B. Fernandez-Dominguez, H. Geissel, M. Gorska, M. Heil, H. T. Johansson *et al.*, Phys. Rev. Lett. **111**, 242503 (2013).
[31] A. Spyrou *et al.*, J. Phys. G: Nucl. Part. Phys. **44**, 044002 (2017).
[32] A. C. Larsen, J. E. Midtbø, M. Guttormsen, T. Renstrøm, S. N. Liddick, A. Spyrou, S. Karampagia, B. A. Brown, O. Achakovskiy, S. Kamerdzhiev, D. L. Bleuel, A. Couture, L. C. Campo, B. P. Crider, A. C. Dombos, R. Lewis, S. Mosby, F. Naqvi, G. Perdikakis, C. J. Prokop *et al.*, Phys. Rev. C **97**, 054329 (2018).
[33] R. Lewis, S. N. Liddick, A. C. Larsen, A. Spyrou, D. L. Bleuel, A. Couture, L. C. Campo, B. P. Crider, A. C. Dombos, M. Guttormsen, S. Mosby, F. Naqvi, G. Perdikakis, C. J. Prokop, S. J. Quinn, T. Renstrøm, and S. Siem, Phys. Rev. C **99**, 034601 (2019).
[34] M. Wiedeking *et al.*, Phys. Rev. Lett. **108**, 162503 (2012).
[35] M. D. Jones, A. O. Macchiavelli, M. Wiedeking, L. A. Bernstein, H. L. Crawford, C. M. Campbell, R. M. Clark, M. Cromaz, P. Fallon, I. Y. Lee, M. Salathe, A. Wiens, A. D. Ayangeakaa, D. L. Bleuel, S. Bottoni, M. P. Carpenter, H. M. Davids, J. Elson, A. Görgen, M. Guttormsen *et al.*, Phys. Rev. C **97**, 024327 (2018).
[36] D. Brink, Doctoral thesis, University of Oxford, 1955.
[37] A. Simon, S. Quinn, A. Spyrou *et al.*, Nucl. Instrum. Methods Phys. Res., Sect. A **703**, 16 (2013).
[38] J. Kopecky and R. Chrien, Nucl. Phys. A **468**, 285 (1987).
[39] A. C. Dombos, D.-L. Fang, A. Spyrou, S. J. Quinn, A. Simon, B. A. Brown, K. Cooper, A. E. Gehring, S. N. Liddick, D. J. Morrissey, F. Naqvi, C. S. Sumithrarachchi, and R. G. T. Zegers, Phys. Rev. C **93**, 064317 (2016).
[40] D. Muecher *et al.* (unpublished).
[41] T. Renstrøm, H.-T. Nyhus, H. Utsunomiya, R. Schwengner, S. Goriely, A. C. Larsen, D. M. Filipescu, I. Gheorghe, L. A. Bernstein, D. L. Bleuel, T. Glodariu, A. Görgen, M. Guttormsen, T. W. Hagen, B. V. Kheswa, Y.-W. Lui, D. Negi, I. E. Ruud, T. Shima, S. Siem *et al.*, Phys. Rev. C **93**, 064302 (2016).
[42] A. V. Voinov, T. Renstrøm, D. L. Bleuel, S. M. Grimes, M. Guttormsen, A. C. Larsen, S. N. Liddick, G. Perdikakis, A. Spyrou, S. Akhtar, N. Alanazi, K. Brandenburg, C. R. Brune, T. W. Danley, S. Dhakal, P. Gastis, R. Giri, T. N. Massey, Z. Meisel, S. Nikas *et al.*, Phys. Rev. C **99**, 054609 (2019).
[43] G. Savard, R. C. Pardo, S. Baker, C. N. Davids, A. Levand, D. Peterson, D. G. Phillips, T. Sun, R. Vondrasek, B. J. Zabransky, and G. P. Zinkann, Hyperfine Interact. **199**, 301 (2011).
[44] C. Harris, M. Smith, A. Spyrou, F. Naqvi *et al.* (unpublished).
[45] R. Schwengner, R. Massarczyk, G. Rusev, N. Tsoneva, D. Bemmerer, R. Beyer, R. Hannaske, A. R. Junghans, J. H. Kelley, E. Kwan, H. Lenske, M. Marta, R. Raut, K. D. Schilling, A. Tonchev, W. Tornow, and A. Wagner, Phys. Rev. C **87**, 024306 (2013).
[46] R. Capote, M. Herman, P. Obložinský, P. Young, S. Goriely, T. Belgya, A. Ignatyuk, A. Koning, S. Hilaire, V. Plujko, M. Avrigeanu, O. Bersillon, M. Chadwick, T. Fukahori, Z. Ge, Y. Han, S. Kailas, J. Kopecky, V. Maslov, G. Reffo *et al.*, Nucl. Data Sheets **110**, 3107 (2009), Special Issue on Nuclear Reaction Data.
[47] A. Koning, S. Hilaire, and M. C. Duijvestijn, TALYS: A nuclear reaction program, NRG Report No. 21297/04.62741/P, also available at http://www.talys.eu.